Energy Conversion and Management 101 (2015) 263–270

Contents lists available at ScienceDirect

Energy Conversion and Management

journal homepage: www.elsevier.com/locate/enconman

Green tide to green fuels: TG–FTIR analysis and kinetic study of *Ulva prolifera* pyrolysis

Selim Ceylan [a,*], Jillian L. Goldfarb [b]

[a] Ondokuz Mayıs University, Faculty of Engineering, Chemical Engineering Department, 55139, Kurupelit, Samsun, Turkey
[b] Boston University, Department of Mechanical Engineering and Division of Materials Science & Engineering, 110 Cummington Mall, Boston, MA 02215, USA

ARTICLE INFO

Article history:
Received 20 February 2015
Accepted 8 May 2015

Keywords:
Algae
Biomass
Pyrolysis
Distributed Activation Energy Model

ABSTRACT

The world grapples with identifying renewable replacements for fossil fuels. *Ulva prolifera*, a macroalgae species that has caused green tides in China and Europe, represents a possible source of renewable energy. Given its low lipid content, thermochemical conversion techniques such as pyrolysis may be more suitable than biochemical techniques. We apply the Distributed Activation Energy Model to determine the activation energy of pyrolysis of *U. prolifera* from thermogravimetric data with combined evolved gas analysis via FTIR. Correlation coefficients for the DAEM were greater than 0.98 at each conversion; the apparent activation energy ranged from 130 to 152 kJ/mol, in good accord with the literature. Three stages of decomposition were noted over the entire temperature range; below 110 °C mass loss due to moisture removal. The largest stage of pyrolysis occurred between 190 and 400 °C with peak mass loss conversion rates up to 8.1 wt% per minute at 20 °C/min. The concentration of CO_2 in the evolved gas peaked along with mass loss rate at 242.7 °C. Stage III of pyrolysis saw a slow mass loss rate and a significant amount of methane from the macroalgae. Given its low energy, nutrient, land and maintenance requirements to grow, tolerance to a variety of environmental conditions, and low pyrolysis activation energies (as compared to other macroalgae), thermochemical conversion via pyrolysis is a viable way to extract energy from this seaweed species.

1. Introduction

A confluence of events in recent history – from unstable oil prices and questionable supply chains, to a rising awareness among the public of the consequences of global warming, to massive green and red tides on multiple continents – have led researchers to investigate the possibility of using various strains of micro- and macroalgae as feedstocks for renewable fuels. Biomass currently supplies upwards of 14% of the world's energy consumption [1]; this number will increase as countries across the globe implement renewable fuel standards in the coming decades [2–4]. There are a multitude of carbonaceous sources from which we can extract energy in many forms, including for power generation, liquid biofuels, and synthetic gas as well as for bio-renewable products such as green chemicals and biochars [5–9]. However, a variety of technical issues plaguing production efficiency, and logistical questions surrounding second-generation feedstock management, have shifted some interest from such solid fuels as agricultural residues onto the possibility of using algae for biofuel production [10,11].

The benefits of using algae as a source for bio-fuels include: year-round production capability; no need for fertilizer or pesticide application; cultivation in fresh or saltwater; no competition for arable land; high photosynthetic capacity and high CO_2 capture efficiency. This is in addition to its considerably higher growth rate and mass productivity than terrestrial lignocellulosic biomass. As an added environmental benefit, owing to its high adsorption capacity, algae grown in wastewater can sequester environmental contaminants while still maintaining biofuel production. An emerging literature has explored the potential use of seaweeds for co-firing to produce electricity, liquid fuel production via thermochemical conversion, and biogas generation via fermentation. [12–17] However, much of the early literature on the extraction of biofuels from algae focused on biochemical conversion pathways, such as extraction and transesterification of the lipids present, rather than thermochemical conversion routes [14]. Given their relatively low amount of fermentable sugars which limits bio-alcohol production, perhaps a more appropriate use for macroalgae is the production of bio-oil via pyrolysis, the thermal conversion of a solid fuel in the absence

* Corresponding author.
E-mail address: selim.ceylan@omu.edu.tr (S. Ceylan).

http://dx.doi.org/10.1016/j.enconman.2015.05.029
0196-8904/

of oxygen to produce a high-energy-density liquid (bio-oil) and relatively low-energy-density gas (bio-gas) [17]. While a plethora of studies exist on the pyrolysis of microalgae, fewer investigations exist on the production of bio-fuels from macroalgae species such as *Ulva prolifera*, a common green seaweed with profusely branching tubular networks widely encountered in intertidal zones of shores and estuaries [18].

Preparations for the 2008 Beijing Olympics were hampered by 20 million wet tons of *U. prolifera* covering over 30% of the area used for the sailing competitions in an unprecedented green tide event [18]. Such blooms are not uncommon; Hu et al. predicts similar aquaculture efforts to be commonplace between May and July in the Yellow and East China Seas [19]. This macroalgae can thrive in a wide range of salinity, water temperatures, and light conditions [20–22], which leads to its often overwhelming environmental presence, but also the facile ability to cultivate it for bio-energy production.

Though studies on the pyrolysis behavior and kinetics of terrestrial biomasses are plentiful, the thermochemical conversion parameters for seaweed biomasses are not as well documented. While the methods used to describe pyrolysis reactions of land-based biomasses are applicable to macroalgae, the differences in composition and plant structure between these biomasses are great, leading to different pyrolytic decomposition profiles [15,23]. The development of efficient thermochemical conversion technologies for biomass to biofuels is required to transform these nascent technologies to commercial scale production [24]. Pyrolysis represents both a direct pathway for conversion of biomass to biofuels, as well as the first step in combustion and gasification reactions. Thus, an improved understanding of the pyrolytic process may assist a variety of thermochemical system designs [25]. For bio-oil production specifically, the relative rates of decomposition, cracking, and repolymerization/condensation reactions, as dictated by heating rates, temperatures and residence times, influence the quantity and quality of the resulting product, as well as the bio-oils' long-term storage stability [26].

Thermogravimetric analysis (TGA) is widely employed in studying the thermal conversion of biomass. TGA enables measurements on the amount and rate of decomposition as a function of temperature and/or time in a controlled atmosphere, providing useful information for designing pyrolysis systems [27]. There are many mathematical models available to describe the pyrolytic decomposition of biomass using isothermal and nonisothermal TGA measurements. The Distributed Activation Energy Model (DAEM), originally proposed by Vand [28], and simplified by Miura [29], assumes that the many heterogeneous chemical reactions occurring during pyrolysis occur simultaneously as irreversible first-order parallel reactions with different rates. The DAEM is widely used to describe the pyrolysis of carbonaceous samples, including studies of a variety of hemicellulosic materials [30], sewage sludge [31], and recently for the study of several aquatic biomasses [32]. Coupling Fourier Transform Infrared (FTIR) spectroscopy to TGA enables measurement of the primary evolved gas products from pyrolysis, which, when combined with mass loss rate information and other kinetic parameters, allows for determination of the optimal pyrolysis temperature(s), heating rates and residence times for targeted volatilization of specific compounds of a given biomass [24].

Turkey owns abundant marine resources, in which seaweeds such as *U. prolifera* are seemingly inexhaustible. This study presents the first pyrolysis analysis of *U. prolifera* using the DAEM. The seaweed was pyrolyzed at three different heating rates, and the DAEM used to estimate its activation energy. FTIR coupled with TGA was employed to characterize the evolved gas products to shed light on the mechanism of thermal decomposition of this prolific strain of macroalgae.

2. Materials and methods

2.1. U. prolifera characteristics

The seaweed biomass used in these experiments, *U. prolifera* (UP), was collected from harbor of Sinop, Turkye, situated on the far northern edge of the Turkish side of the Black Sea coast. The samples were rinsed with deionized water to remove surface dirt, dried in a 60 °C oven overnight, crushed, and sieved to a particle size of 63–125 μm. It was shown that particles of this size and smaller, with Biot numbers considerably less than 1, do not suffer from heat and/or mass transfer limitations during pyrolysis [7]. Proximate analysis was performed on a TGA and the results present in Table 1. The sample's moisture was obtained after achieving constant weight at 110 °C in an inert atmosphere. The volatile carbon content was determined by heating the sample to 950 °C in an inert atmosphere. The carbon-mineral distribution was determined by heating the sample in air; the fixed carbon was represented by loss after an isothermal process at 550 °C and the ash content was the amount remaining after high-temperature oxidation at 550 °C. The ultimate analysis was carried out in a LECO TruSpec CHN elemental analyzer.

2.2. Thermogravimetric analysis

Thermogravimetric analysis (TGA) was carried out using Simultaneous Differential Thermogravimetric Analyzer (DTA) equipped with a heat-flux type DTA and a TGA (Shimadzu, DTG-60, Japan; with a precision of temperature measurement ±0.1 K, DTA sensitivity ±0.1 μV and microbalance sensitivity ±0.1 μg) at heating rates of 5, 10, and 20 °C min^{-1} under a nitrogen atmosphere with a flow rate of 80 mL min^{-1} with samples of approximately 10 mg. Once the sample was introduced in the TGA, the temperature was raised from ambient temperature to 110 °C and maintained for 20 min to ensure moisture removal. Then the temperature was ramped to 1000 °C at the specified heating rate under continuous nitrogen. Non-isothermal TGA is widely applied to obtain the kinetic parameters of the thermochemical conversion of biomass. In comparison to isothermal TGA experiments, non-isothermal experiments are considered to be more reliable to perform because there is a weight loss associated with reaching desired isotherms, leading to erroneous calculations of kinetic parameters [33].

2.3. TGA–FTIR analysis

The TGA–FTIR experiments were carried out in a thermogravimetric analyzer coupled with Fourier transform infrared spectrometry (Perkin Elmer Pyris Simultaneous Thermal Analysis (STA)

Table 1
Proximate and ultimate analysis of *Ulva prolifera* (dry, ash-free basis).

Proximate analysis (% w/w)	
Moisture	9.92
Volatile matter	57.87
Fixed carbon	7.77
Ash	24.46
Ultimate analysis (% w/w)	
C	37.44
H	7.01
N	1.87
S	2.88
O[a]	50.8
H/C	0.19
O/C	1.14
Higher heating value (MJ/kg)	16.54

[a] Calculated by difference.

600). Approximately 10 mg of UP was loaded onto the sample holder for each run. The samples were heated from ambient temperature to 800 °C at a heating rate of 20 °C min^{-1}. The flow rate of the carrier inert gas (high purity nitrogen) was 50 mL min^{-1}. The spectral region of the FTIR was 4000–400 cm^{-1} and spectrum scan was conducted with 0.12 s intervals.

2.4. Kinetic analysis via distributed activation energy analysis model

The Distributed Activation Energy Model is generally regarded as a convenient method to analyze the kinetics of biomass pyrolysis, showing excellent agreement with the experimental data at lower heating rates. Therefore, these data are widely applicable to a range of pyrolysis conditions to produce bio-oil, as well as in studying the latter-stages of char burnout for industrial applications where reactivities in industrial boilers are in within Zone I kinetic regimes [34,35].

The DAEM assumes the existence of an infinite number of parallel irreversible first order reactions that occur simultaneously, each with different activation energies, *E*. The DAEM method assumes that all the reaction activation energies have the same pre-exponential factor, k_0, at the same conversion rate, and that the activation energy has a continuous distribution. The DAEM represents the change in total volatiles of a solid as:

$$1 - V/V^* = \int_0^\infty exp\left(-\frac{k_0}{\beta}\int_0^t e^{-E/RT}dT\right)f(E)dE \quad (1)$$

where V is the volatile content at absolute temperature *T* with heating rate β, V^* is the effective volatile content of the solid, k_0 is the frequency factor corresponding to a given E value. f(E) is the distribution curve of the activation energy that encapsulates the range and variation in the activation energies of the simultaneous first-order irreversible reactions and, is normalized as:

$$\int_0^\infty f(E)dE = 1 \quad (2)$$

The distribution function can be used to simplify Eq. (1), representing the normalized distribution of activation energies across all possible irreversible reactions as:

$$\frac{V}{V^*} = 1 - \int_{E_S}^\infty f(E)dE = \int_0^{E_S} f(E)dE \quad (3)$$

where E_s is the activation energy at a given temperature. The Arrhenius equation assumes the form [36]:

$$\ln\left(\frac{\beta}{T^2}\right) = \ln\left(\frac{k_0 R}{E_s}\right) + 0.6075 - \frac{E_s}{RT} \quad (4)$$

The values of the activation energy, E_s, and corresponding frequency factor in Eq. (4) are obtained from three separate TGA curves, each with their own heating rate, by plotting the natural log of (a/T^2) versus inverse temperature at selected conversion (V/V^*) values for different heating rates. Thus, the activation energy obtained from the Arrhenius plots of Eq. (4) represent different levels of solid pyrolysis decomposition.

3. Results and discussion

3.1. Characterization of UP

The proximate and ultimate analysis and higher heating value of UP are shown in Table 1, taken after drying the samples at 60 °C overnight. The volatile matter content was 57.87%, similar to other macroalgae species, such as 55.6% for *Chlorococcum humicola* [37], 57.99% for *Enteromorpha clathrata*, 44.85% for *Sargassum natans* [23], 68.79% for *Saccharina japonica* [38], and 44.50% for *A. Sagarassum* [39]. A high volatile matter content is desirable for formation of gas and liquid products via pyrolysis. The higher heating value of *U. prolifera* was higher than some other macroalgae [38,39]. This can be attributed to higher C and H contents in *U. prolifera*. The moisture content in UP was 9.92%. Such a high moisture ratio is not desirable when transportation and heating values are considered, though this is not dissimilar in magnitude to many biomass source currently being considered for conversion to bio-oils via pyrolysis. It is proposed that in a bio-refinery concept, waste heat from pyrolysis gas combustion could be used to dry the incoming biomass to reduce this moisture content if necessary.

High ash content, measured for UP as 23.51%, is common among seaweeds due to their biosorption of mineral compounds, and can reduce the efficiency of thermochemical systems [15]. Ash can limit heat and mass transfer while creating problems such as agglomeration, slagging, and fouling in boilers [40]. The nitrogen content in UP was relatively low (1.87%), as compared to other seaweed strains such as *E. clathrata* and *S. natans* at 3.14% and 3.58%, respectively, though not as low as observed concentrations in *Gracilaria cacalia* at 0.83% [38] and *S. japonica* at 0.93% [38]. In biomass pyrolysis, nitrogen leads to formation of NO_x precursors (NH_3 and HCN) [41,42]; lower N ratios are therefore favorable. However, UP has a high S ratio, 2.88%, which can cause environmental problems and corrosion in reactors.

The FTIR spectrum of raw *U. prolifera* is shown in Fig. 1 with bands assigned according to literature [43–46], summarized in Table 2. The large peak at 3365 cm^{-1} is attributed to the stretching of primarily –OH groups, but possibly also of N—H. However, given its broad, strong nature, the former is more likely. The stretching associated with the peak at 2925 cm^{-1} of C—H is suggestive of a lipid's methylene group [42]. However, the identification of this peak is somewhat problematic due to the presence of the small peak at 1223 cm^{-1}, and the superposition of overlapping bonds, possibly of ether, epoxide or phenolic structures [41]. Given the known high lipid *and* phenolic content of algal biomass, we suspect that these are overlapping contributors to the peaks at 2925 and 1223 cm^{-1} [45]. The strong, intense peak at 1640 cm^{-1} is thought to correspond to C=O amide stretching from proteins present in algae [46]. The peak spanning 1425–1417 cm^{-1} is likely indicative of C—H stretching vibration in methyl, methylene and methyne groups. The peak at 1324 cm^{-1} is thought to be the C—O stretching of organic acids. The twin absorbance peaks at 1035 cm^{-1} and 1003 cm^{-1} are likely the C—O and C—O—H deformation in secondary and primary alcohols or aliphatic ethers and, according to

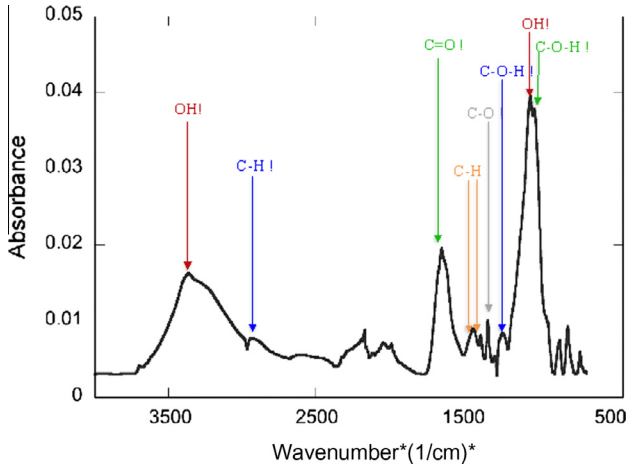

Fig. 1. FTIR spectra of *Ulva prolifera* prior to pyrolysis with primary peaks corresponding to labels in Table 2.

Table 2
Functional groups as assigned to specific wavenumbers for FTIR analysis of raw *Ulva prolifera* and gases devolatilizing during pyrolysis [43–46].

Functional group	Wavenumber (cm^{-1})	Assigned species
Functional groups in devolatilized gases from Ulva prolifera pyrolysis		
O—H	4000–3400	H_2O
C—H	3000–2700	CH_4
C═O	2400–2250	CO_2
C—O	2250–2000	CO
C═O	1900–1650	Aldehydes, ketones, acids
C═C	1690–1450	Aromatics
C—O, C—C	1475–1000	Alkanes, alcohols, phenols, ethers, lipids
Fingerprint region of 1475–1000		
C—H, C—C	1460–1365	Alkanes
C—O	1300–1200	Phenols
C—O	1300–1050	Lipids
C—O	1275–1060	Ethers
C—O	1200–1000	Alcohols
C═O	586–726	CO_2
Functional groups assigned to peaks on solid Ulva prolifera surface		
—OH, N—H	3365	Alcohol, amine
C—H	2925	Methylene group (lipids)
C═O	1640	Aromatic conjugate
$—CH_3$	1425–1417	Methyl, methylene, methyne
C—O	1324	Acid
C—O—H	1223	Phenols
C—O; C—O—H	1035–1005	Alcohols, esters, polysaccharides

Mahapatra and Ramachandra [46], the second of these may indicate the vibrational stretching of C—O—H from polysaccharides.

3.2. Kinetics of thermal decomposition

Samples of *U. prolifera* were pyrolyzed in an inert nitrogen atmosphere at 5, 10 and 20 °C/min; the TG and DTG curves are presented in Fig. 2a and b, respectively. As seen throughout the literature on micro- and macroalgae pyrolysis, there are three primary stages of pyrolysis as highlighted by the DTG [47–53]. The first, from room temperature until 120 °C, is attributed to moisture removal (both surface and entrained water) of the sample. The sharp DTG peak, representing the primary pyrolysis or Stage II, began between 196 and 208 °C and finished between 295 and 320 °C, as given in Table 3. Within Stage II, *U. prolifera* devolatilized approximately 45 wt% of its total sample mass. The peak mass loss temperature and rate of mass loss, as seen in Fig. 2b, increased as the heating rate increased. Peak temperature and heating rate are linearly correlated with a correlation coefficient of $R^2 = 0.9963$, whereas the peak mass loss rate follows a similar trend though with a correlation coefficient of only $R^2 = 0.8519$. In previous studies, this shift in thermal profiles was attributed to heat and mass transfer limitations that become exacerbated at higher heating rates, when the reaction time of the samples decreases. At the higher heating rate, the extent of the pyrolysis reaction at any given temperature is lower than its slower counterparts. Given the small particle size and sample size used, it is unlikely that there is a large temperature gradient within each particle or sample (the $Bi \ll 1$ and therefore lumped capacitance is a reasonable assumption). A more likely explanation for the impact of heating rate is the residence time at each temperature stage; the particles devolatilize more slowly but over a longer time at lower heating rates, accounting for the same total mass fraction conversion, but variance in temperature and mass loss rates.

It is for these reasons that the Distributed Activation Energy Model is often employed in biomass pyrolysis; by incorporating data over a series of heating rates, we can "average out" the effect of heating rate and obtain a global apparent activation energy for

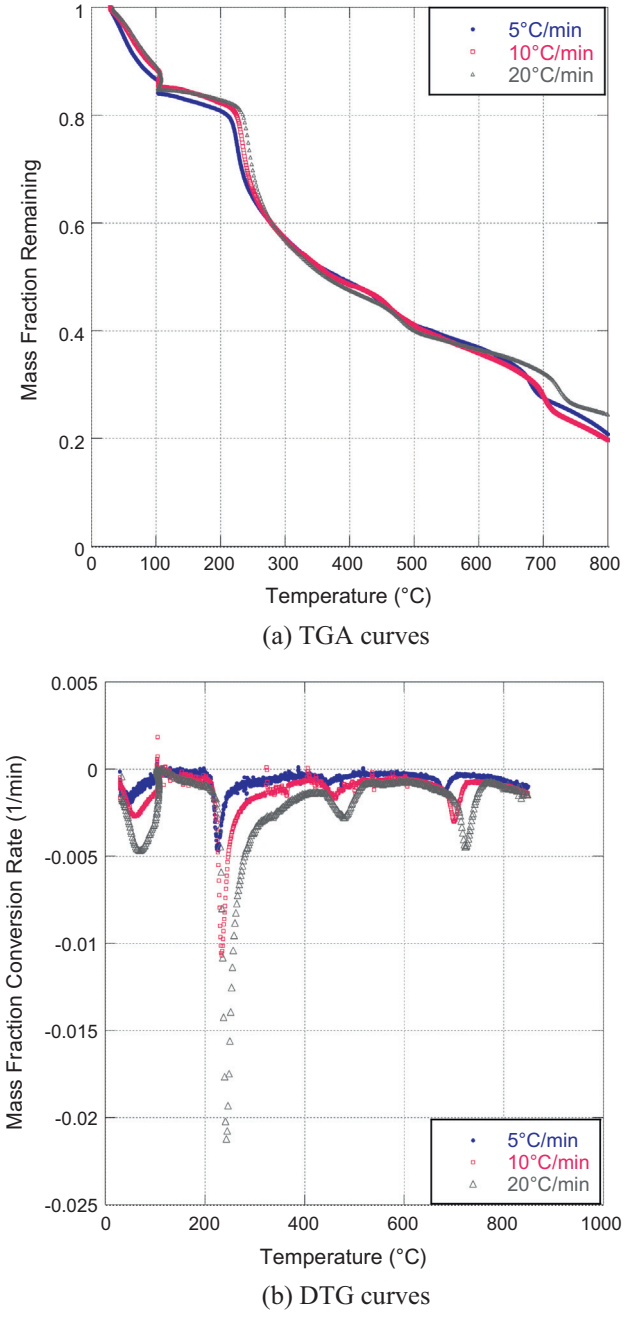

Fig. 2. Thermogravimetric data for pyrolysis of *Ulva prolifera* at different heating rates 5 °C/min (●); 10 °C/min (□); 20 °C/min (△).

Table 3
Thermal degradation characteristics of *Ulva prolifera* at different heating rates.

Heating rate, °C min^{-1}	T_i, °C	T_f, °C	DTG_{max}, % min^{-1}	T_{max}, °C	$R_M \times 10^3$, % min^{-1} °C^{-1}
5	196	295	3.1	224	13.89
10	201	311	6.5	229	28.38
20	208	320	8.1	242	33.47

the material. Table 4 presents the correlation equations and coefficients obtained using Eq. (4) and the isoconversional plots of Fig. 3, and the resulting activation energies and frequency factors at each conversion level. As the correlation coefficients (R^2) for each conversion point are greater than 0.98, we are confident that the DAEM and its assumption of multiple simultaneous first order

Table 4
Fitted equations and correlation coefficients with resulting activation energies and frequency factors for *Ulva prolifera* pyrolysis obtained by the Distributed Activation Energy Model.

Conversion	Equation	Correlation	E, kJ/mol	k_0, s^{-1}
0.1	$y = -15664x + 19.488$	$R^2 = 0.9972$	130.23	2.48E+12
0.2	$y = -15797x + 19.012$	$R^2 = 0.9823$	131.33	1.55E+12
0.3	$y = -16220x + 18.961$	$R^2 = 0.9807$	134.85	1.52E+12
0.4	$y = -17548x + 23.671$	$R^2 = 0.9986$	145.89	1.82E+14
0.5	$y = -17460x + 23.870$	$R^2 = 0.9999$	145.16	2.21E+14
0.6	$y = -18782x + 26.778$	$R^2 = 0.9997$	151.51	4.36E+15
0.7	$y = -18224x + 25.969$	$R^2 = 0.9988$	152.41	1.88E+15
0.8	$y = -16759x + 23.474$	$R^2 = 0.9990$	139.33	1.41E+14

decomposition reactions is a reasonable model for the prediction of activation energies of pyrolysis of *U. prolifera*. The activation energy for pyrolysis ranges from 130 to 152 kJ/mol, with an average value of 141.34 ± 8.71 kJ/mol. The apparent activation energy values vary with conversion as the pyrolytic decomposition proceeds, underscoring the complex mechanisms of pyrolysis that change as the composition of the material changes. However, as Fig. 4 demonstrates, we find good agreement between TG curves calculated using the kinetic parameters obtained from the DAEM and the measured data at each heating rate. As such, we are confident in the applicability of the DAEM to describe the complex pyrolysis reactions of UP degradation.

The activation energy measured here compares favorable to activation energies of pyrolysis of micro- and macroalgae species seen throughout the literature, as detailed in Table 5. The

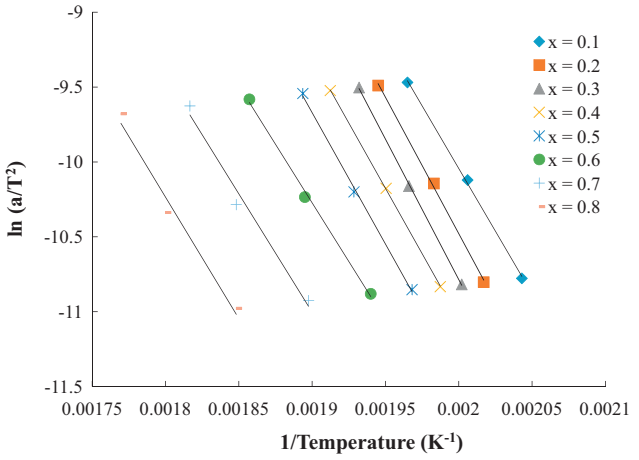

Fig. 3. Isoconversional plot for determination of activation energy of pyrolysis of *Ulva prolifera* via the Distributed Activation Energy Model.

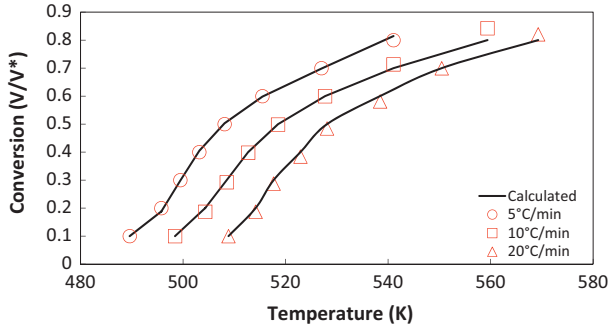

Fig. 4. Simulated versus experimental data for 5 (○), 10 (□) and 20 (△) °C/min pyrolysis of *Ulva prolifera*.

activation energy measured for *U. prolifera* is quite similar to another macroalgae within the same genus, *Ulva pertusa*, a recent introduction to – and potentially invasive species in – the Mediterranean Sea as a result of oyster transfers from the Pacific Ocean [57]. The activation energy of *U. pertusa* was calculated to be 148.7 kJ/mol via an average of the Flynn–Wall–Ozawa, Kissinger–Akahira–Sunose and Popescu methods [50]. Some microalgae have activation energies as low as 46 kJ/mol [52], others, such as *Spiruline plantensis*, have activation energies upwards of 100 kJ/mol. The majority of the macroalgae species with data in the literature have activation energies of pyrolysis upwards of 140 kJ/mol, some reported as high as 228.09 (*Enteromorpha prolifera*) [55], making *U. prolifera* a reasonable candidate for bio-fuel production via pyrolysis, as compared to many other species. Given its kinetic potential for use as a bio-fuel, we turned our attention next to an analysis of the evolved gas from pyrolysis as monitored by FTIR to guide discussion of the changing nature of the pyrolysis reactions as a function of temperature, important to understanding how to optimize the process for fuel recovery.

3.3. Evolved gas analysis

Volatile compounds evolved during the thermal decomposition of UP were analyzed in real time by FTIR. Fig. 5 presents the IR spectra taken at peak temperatures as observed in the DTG curve obtained at 20 °C min^{-1}; the assigned peaks correspond to the functional groups detailed in Table 2 according to the literature. The split plots – one at the low temperature points of 242.7 and 487.7 °C, the second at the higher temperatures of 684.0 and 800.0 °C – provide a semi-quantitative description of the reaction coordinate. At lower temperatures we see weaker absorbance signals with the most significant peaks between 2400 and 2270 cm^{-1}. These, as noted in Table 2, are ascribed to the C=O stretching of CO_2. The absorbance between these wavenumbers is considerably less than other species at higher temperatures. Ma et al. noted similar behavior during the pyrolysis of palm kernel shell [43], and Meng et al. found such behavior during the pyrolysis of corn cob, sugar cane bagasse, and tree root [58].

At each measurement temperature we see the characteristics signals of water between 4000 and 3400 cm^{-1}; the absorbances are actually slightly higher for higher temperatures (between 0.004 and 0.01 at 800 °C) than lower temperatures (less than 0.002), though given the scale of Fig. 5 this is not immediately obvious. The surface-bound and entrained moisture were likely removed at the isothermal hold at 110 °C. The mass loss at 242.7 °C is likely a function of devolatilization and further removal of entrained water, as opposed to the ring-opening, depolymerization, recondensation and repolymerization, reactions occurring at higher temperatures. Such reactions occurring at higher temperatures explain both the presence of more water at higher temperatures, and the increase in activation energy as conversion increases as such reactions require more energy to overcome the barrier to reaction [47].

The absorbance bands between 1750 and 1650 cm^{-1} with peaks at 1710 (242.7 and 487.7 °C) and 1740 (684.0 and 800.0 °C) correspond to the C=O carbonyl stretching of carboxylic acid, ketones, or aldehyde groups. It is most likely that these signals represent carboxylic groups. Carboxylic acids are commonly identified in macroalgae, However, further evidence is the peak at 1740 cm^{-1} observed at higher temperatures, likely indicative of ester species, which form from the combination of carboxylic acids and alcohols, observed in the fingerprint region between 1200 and 1000 cm^{-1} [22].

At 487.7 °C we see a relatively large peak at 1250 cm^{-1}, absent from the other temperatures, which lays in the fingerprint region

Table 5
Survey of activation energies of marine biomass pyrolysis available in the literature.

Marine biomass	Activation energy, kJ/mol	Kinetic analysis method	Reference
Chlorella protothecoides	46.2	Average of Freeman-Carroll at 15, 40, 60, 80 °C/min	[52]
Chlorella pyrenoidosa	77.02[a]	Iso-conversional	[47]
Chlorella pyrenoidosa	100.06	Distributed Activation Energy Model	[12]
Chlorella sorokiniana	108.63	Distributed Activation Energy Model	[32]
Chlorella spp.	71.3–79.2	Freeman-Carroll	[51]
Chlorococcum humicola	189.99	Distributed Activation Energy Model	[37]
Corallina pilulifera	247.7	Average of: Flynn–Wall–Ozawa, Kissinger–Akahira–Sunose; Popescu	[54]
Dunaliella tertiolecta	146.07	Average of Isoconversional: Flynn–Wall–Ozawa, Kissinger–Akahira–Sunose	[27]
Dunaliella tertiolecta	186.46[b]	Iso-conversional	[53]
Dunaliella tertiolecta	171.85[b]	Iso-conversional	[53]
Enteromorpha prolifera	228.09	Average of Freeman-Carroll at 10; 20; 50 °C/min	[55]
Enteromorpha prolifera	178.89[b]	Iso-conversional	[53]
Laminaria japonica	207.7	Average of: Flynn–Wall–Ozawa, Kissinger–Akahira–Sunose; Popescu	[56]
Plocamium telfairiae	249.1	Average of: Flynn–Wall–Ozawa, Kissinger–Akahira–Sunose; Popescu	[54]
Pophyra yezoensis	157.3	Average of: Flynn–Wall–Ozawa, Kissinger–Akahira–Sunose; Popescu	[54]
Saccharina japonica	168.3	Average of nonlinear least-squares of first order kinetics (Arrhenius)	[38]
Sargassum pallidum	202.9	Average of: Flynn–Wall–Ozawa, Kissinger–Akahira–Sunose; Popescu	[56]
Sargassum thunbergii	140.1	Average of: Flynn–Wall–Ozawa, Kissinger–Akahira–Sunose; Popescu	[49]
Spirulina platensis	91.56[a]	Iso-conversional	[47]
Spirulina platensis	100.11	Average of first order Arrhenius equation, 5; 10; 20; 30 °C/min	[48]
Spirulina platensis	83.1	Average of Freeman-Carroll at 15, 40, 60, 80 °C/min	[52]
Ulva pertusa	148.7	Average of: Flynn–Wall–Ozawa, Kissinger–Akahira–Sunose; Popescu	[50]
Ulva prolifera	141.34 ± 8.71	Distributed Activation Energy Model	This work

[a] Average of multiple conversion values supplied by authors.
[b] Representative of Zone 2 conversion, primary mass loss regime.

of C—O stretching, indicating the presence of either phenols or lipids; we imagine this is more likely attributable to both species, though macroalgae are known to have a comparably high phenolic versus lipid content [59]. Finally of note is the characteristic peak of CH_4 associated with C—H stretching between 3000 and 2860 cm^{-1} observed at the two highest temperatures, with orders of magnitude less observed at lower temperatures.

Fig. 6 presents the relative peak concentrations of C=O, and C—O groups, along with H_2O and CH_4 as a function of temperature, along with mass fraction converted. The absorbance, which is of course directly related to concentration in the gas phase, is presented on a log scale such that we can easily differentiate orders of magnitude of each component evolved at a given temperature and decomposition stage. The primary devolatilization of the UP

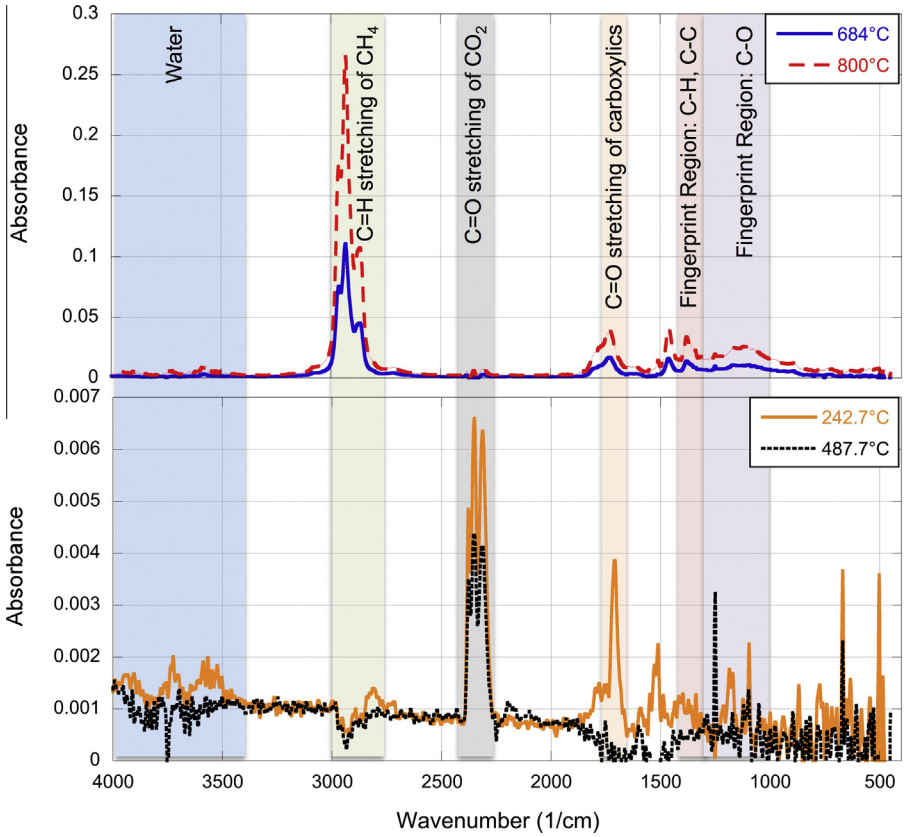

Fig. 5. FTIR spectra of UP pyrolyzed at 20 °C/min at 242.7 °C (solid); 487.7 °C (**dotted**); 684.0 °C (solid); 800.0 °C (dashed).

in terms of overall mass conversion occurred above 242.7 °C and below 684.0 °C – between these two temperatures the mass fraction converted goes from approximately one quarter to three quarters. However, the composition of the evolving gases clearly changes over this temperature range. Despite only loosing 10% of the mass between 684 and 800 °C, the concentrations of water and CH_4 evolved increase by orders of magnitude above the lower temperature measurements. This may seem, initially, counter-intuitive; how can gaseous products evolved be high when the overall conversion is in fact slowing down? The FTIR analysis is focused only on the pyrolysis gases, and not the liquid (condensable) bio-oils, nor on any tars condensing within the structure of the remaining UP char, or the char itself. As temperature increases, the solid residue decomposes slowly, forming a porous residue [54], which in the case of UP will involve the condensing of carbon into the mineral matter naturally present in the macroalgae. Maximum liquid yields from pyrolysis are known to occur around 500 °C under limited vapor residence times conditions to prevent secondary reactions [60,61]. As has been noted for both terrestrial and aquatic biomasses, above this point gaseous yields increase and solid char yields decreases, accompanied by the release of gases such as CO and CO_2; the dominance of CO_2 over CO is know to differentiate algae from lignocellulosic biomass pyrolysis [61–67]. As such, the peak concentrations of pyrolysis gas species such as CH_4 occur at higher temperatures, whereas the condensable liquid species would be maximized between the highest conversion temperatures.

While macroalge lack the lignocellulosic structures of terrestrial biomasses, instead characterized by their protein, carbohydrate and lipid components, along with higher contents of alkali earth metals, halogens, carbonates and other inorganics [68,69], the pyrolytic behavior of both types of biomasses are quite similar. Though the concentrations of metals in the seaweeds lead to higher ash contents, the trade-off to their presence is their potential catalytic activity during pyrolysis. The presence of inorganic materials has been shown to promote secondary cracking reactions in the gas phase, and that the presence of minerals in biomass decreases the peak decomposition temperatures and volatile yields [70–72]. It is also because of this relatively high mineral matter composition that the renewable energy conversion of macroalgae such as *U. prolifera* via combustion or gasification is less desirable, due to slagging and fouling issues, than pyrolysis to produce liquid and/or gaseous bio-fuels.

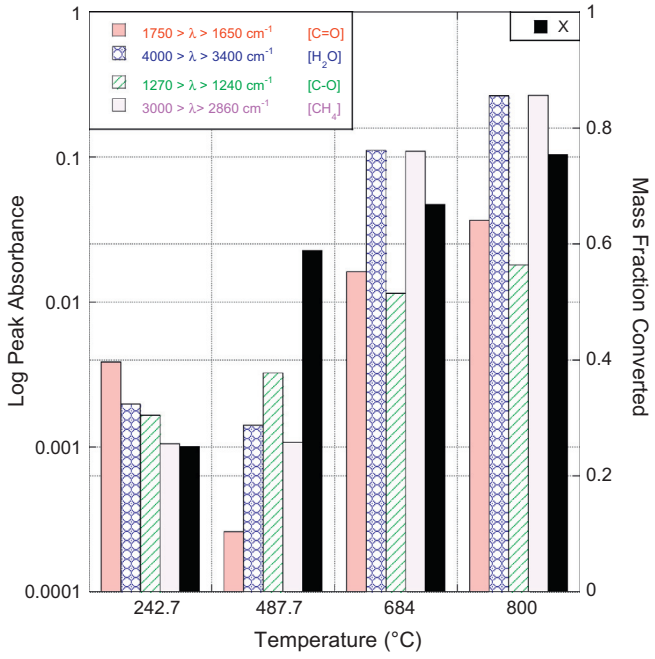

Fig. 6. (Log) peak absorbance as a function of temperature and corresponding conversion for: (□) carboxylic groups; (▨) water; (▨) phenols/lipids; (□) CH_4.

4. Conclusions

The Distributed Activation Energy Model was used to determine the activation energy of pyrolysis of *U. prolifera* from thermogravimetric data at three different heating rates (5, 10, 20 °C/min). The model assumes the decomposition mechanism takes a large number of independent, parallel reactions with different activation energies reflecting variations in the bond strengths of species whose activation energies can be continuously distributed as a function of conversion. Correlation coefficients for the DAEM were all greater than 0.98 at each conversion level, and resulting values of the apparent activation energy ranged from 130 to 152 kJ/mol, in good accord with the literature. Three stages of decomposition were noted over the entire temperature range; below 110 °C mass loss was due primarily to moisture removal. The largest stage of pyrolysis occurred between 190 and 400 °C with peak mass loss conversion rates up to 8.1 wt% per minute at 20 °C/min pyrolysis. Above 400 °C we see slow a slow mass loss rate of less than 10% of the total sample mass.

The peak conversion rate at 20 °C/min occurred at 242.7 °C. At this temperature, evolved gas analysis via FTIR showed significant quantities of CO_2 present, as well as signatures of C=O stretching likely associated with carboxylic acid presence. This peak diminishes slightly at 487.7 °C, where we see evidence of phenolic species devolatilizing. At higher temperatures, during Stage III of pyrolysis (slow mass loss rates, likely a result of cracking and condensation reactions) a significant absorbance between 3000 and 2860 cm^{-1} indicated a large amount of methane devolving from the macroalgae. This peaked around 800 °C, when CO_2 was at a minimum.

Overall, the potentially invasive seaweed species that has caused newsworthy green tides in Asia and Europe, *U. prolifera*, may well be a potential source of bio-renewable fuels. Given its low energy, nutrient, land and maintenance requirement to grow, tolerance to a variety of environmental conditions, its low pyrolysis activation energies (as compared to other macroalgae), thermochemical conversion via pyrolysis is a viable way to extract energy from this species. Results indicate that maximum conversion temperatures occur as low as 240 °C, and the composition of the gas produced can be altered via pyrolysis temperature. Further studies on the analysis of bio-oil obtainable from pyrolysis of *U. prolifera* are recommended.

References

[1] Saxena RC, Adhikari DK, Goyal HB. Biomass-based energy fuel through biochemical routes: a review. Renew Sustain Energy Rev 2009;13:167–78.
[2] United States Energy Independence and Security Act (EISA) of 2007. Public Law 110–140. <http://www.gpo.gov/fdsys/pkg/BILLS-110hr6enr/pdf/BILLS-110hr6enr.pdf> [accessed 14.02.15].
[3] Wiesenthal T, Leduc G, Christidis P, Schade B, Pelkmans L, Govaerts L, et al. Biofuel support policies in Europe: lessons learnt for the long way ahead. Renew Sustain Energy Rev 2009;13:789–800.
[4] Matsumoto N, Sano D, Elder M. Biofuel initiatives in Japan: strategies, policies, and future potential. Appl Energy 2009;86:S69–76.
[5] Soria-Verdugo A, Garcia-Hernando N, Garcia-Gutierrez LM, Ruiz-Rivas U. Analysis of biomass and sewage sludge devolatilization using the distributed activation energy model. Energy Convers Manage 2013;65:239–44.
[6] Ceylan S, Topçu Y. Pyrolysis kinetics of hazelnut husk using thermogravimetric analysis. Bioresour Technol 2014;156:182–8.
[7] Buessing L, Goldfarb JL. Energy along interstate I-95: pyrolysis kinetics of Floridian cabbage palm (*Sabal palmetto*). J Anal Appl Pyrol 2012;96:78–85.
[8] Mérida W, Maness P-C, Brown RC, Levin DB. Enhanced hydrogen production from indirectly heated, gasified biomass, and removal of carbon gas emissions using a novel biological gas reformer. Int J Hydrogen Energy 2004;29:283–90.

[9] Sanna A, Li S, Linforth R, Smart KA, Andrésen JM. Bio-oil and bio-char from low temperature pyrolysis of spent grains using activated alumina. Bioresour Technol 2011;102:10695–703.
[10] Naik SN, Goud VV, Rout PK, Dalai AK. Production of first and second generation biofuels: a comprehensive review. Renew Sustain Energy Rev 2010;14:578–97.
[11] Bird MJ, Wurster CM, de Paula Silva PH, Bass AM, de Nys R. Algal biochar – production and properties. Bioresour Technol 2011;102:1886–91.
[12] Hu M, Chen Z, Guo D, Liu C, Xiao B, Hu Z, et al. Thermogravimetric study on pyrolysis kinetics of *Chlorella pyrenoidosa* and bloom-forming cyanobacteria. Bioresour Technol 2015;177:41–50.
[13] Posten A, Schaub G. Microalgae and terrestrial biomass as source for fuels – a process view. J Biotechnol 2009;142:64–9.
[14] Amin S. Review on biofuel and gas production processes for microalgae. Energy Convers Manage 2009;50:1834–40.
[15] Yanik J, Stahl R, Troeger N, Sinag A. Pyrolysis of algal biomass. J Anal Appl Pyrol 2013;103:134–41.
[16] Ali SAM, Razzak SA, Hossain MM. Apparent kinetics of high temperature oxidative decomposition of microalgal biomass. Bioresour Technol 2015;175:569–77.
[17] Choi J, Choi J-W, Suh DJ, Ha J-M, Hwang JW, Jung HW, et al. Production of brown algae pyrolysis oils for liquid biofuels depending on the chemical pretreatment methods. Energy Convers Manage 2014;86:371–8.
[18] Gao S, Chen X, Yi Q, Wang G, Pan G, Lin A, et al. A strategy for the proliferation of *Ulva prolifera*, main causative species of green tides, with formation of sporangia by fragmentation. PLoS ONE 2010;5:e8571.
[19] Hu C, Li D, Chen C, Ge J, Muller-Karger FE, Liu J, et al. On the recurrent *Ulva prolifera* blooms in the Yellow Sea and East China Sea. J Geophys Res 2010;115:C05017.
[20] Callow ME, Callow JA. Primary adhesion of *Entermorpha* (Chlorophyta, Ulvales) propagules: quantitative settlement studies and video microscopy. J Phycol 1997;33:938–47.
[21] Taylor D, Nixon S, Granger S, Buckley B. Nutrient limitation and the eutrophication of coastal lagoons. Mar Ecol Prog Ser 1995;127:235–44.
[22] Nelson TA, Haberlin K, Nelson AV, Ribaric H, Hotchkiss R, van Alstyne KL, et al. Ecological and physiological controls of species composition in green macroalgal blooms. Ecology 2008;89:1287–98.
[23] Wang S, Wang Q, Jiang X, Han X, Ji H. Compositional analysis of bio-oil derived from pyrolysis of seaweed. Energy Convers Manage 2013;68:273–80.
[24] Bassilakis R, Carangelo RM, Wójtowicz. TG–FTIR analysis of biomass pyrolysis. Fuel 2001;80:1765–86.
[25] Bridgwater AV. Renewable fuels and chemicals by thermal processing of biomass. Chem Eng J 2003;91:87–102.
[26] Mohan D, Pittman Jr CU, Steele PH. Pyrolysis of wood/biomass for bio-oil: a critical review. Energy Fuels 2006;20:848–89.
[27] Shuping Z, Yulong W, Mingde Y, Chun L, Junmao T. Pyrolysis characteristics and kinetics of the marine microalgae *Dunaliella tertiolecta* using thermogravimetric analyzer. Bioresour Technol 2010;101:359–65.
[28] Vand V. A theory of the irreversible electrical resistance changes of metallic films evaporated in vacuum. Proc Phys Soc 1943;55:222.
[29] Miura K. A new and simple method to estimate f(E) and k0(E) in the Distributed Activation Energy Model from three sets of experimental data. Energy Fuels 1995;9:302–7.
[30] Cai J, Wu W, Liu R, Hubert GW. A distributed activation energy model for the pyrolysis of lignocellulose biomass. Green Chem 2013;15:1331–40.
[31] Soria-Verduge A, Garcia-Hernando N, Garcia-Gutierrez LM, Ruiz-Rivas U. Pyrolysis of biomass and sewage sludge devolatilization using the distributed activation energy model. Energy Convers Manage 2013;65:239–44.
[32] Yang X, Zhang R, Fu J, Geng S, Cheng JJ, Sun Y. Pyrolysis kinetics and product analysis of different microbial biomass by distributed activation energy model and pyrolysis–gas chromatography–mass spectrometry. Bioresour Technol 2014;163:335–42.
[33] Mishra G, Bhaskar T. Non isothermal model free kinetics for pyrolysis of rice straw. Bioresour Technol 2014;169:614–21.
[34] Chan ML, Jones JM, Pourkashanian M, Williams A. The oxidative reactivity of coal chars in relation to their structure. Fuel 1999;78:1539–52.
[35] Jones JM, Bridgeman TG, Darvell LI, Gudka B, Saddawi A, Williams A. Combustion properties of torrefied willow compared with bituminous coal. Fuel Process Technol 2012;101:1–9.
[36] Munir S, Daood S, Nimmo W, Cunliffe A, Gibbs B. Thermal analysis and devolatilization kinetics of cotton stalk, sugar cane bagasse and shea meal under nitrogen and air atmospheres. Bioresour Technol 2009;100:1413–8.
[37] Kirtania K, Bhattacharya S. Application of the distributed activation energy model to the kinetic study of the fresh water algae *Chlorococcum humicola*. Bioresour Technol 2012;107:476–81.
[38] Kim S-S, Ly HV, Choi G-H, Kim J, Woo HC. Pyrolysis characteristics and kinetics of the alga *Saccharina japonica*. Bioresour Technol 2012;123:445–51.
[39] Kim S-S, Ly HV, Choi JH, Woo HC. Thermogravimetric characteristics and pyrolysis kinetics of Alga *Sagarssum* sp. Biomass Bioresour Technol 2013;139:242–8.
[40] Wang S, Jiang XM, Han XX, Wang H. Fusion characteristic study on seaweed biomass ash. Energy Fuels 2008;22:2229–35.
[41] Ren Q, Zhao C, Chen X, Duan L, Li Y, Ma C. NO_x and N_2O precursors (NH_3 and HCN) from biomass pyrolysis: Co-pyrolysis of amino acids and cellulose, hemicellulose, and lignin. Proc Combust Inst 2011;33:1715–22.
[42] Becida M, Skreiberg Ø, Hustad JE. NO_x and N_2O precursors (NH_3 and HCN) in pyrolysis of biomass residues. Energy Fuels 2007;21:1173–80.
[43] Ma Z, Chen D, Gu J, Bao B, Zhang Q. Determination of pyrolysis characteristics and kinetics of palm kernel shell using TGA–FTIR and model-free integral methods. Energy Convers Manage 2015;89:251–9.
[44] Gupta VK, Rastogi A. Biosorption of hexavalent chromium by raw and acid-treated green alga *Oedogonium hatei* from aqueous solution. J Hazard Mater 2009;163:396–402.
[45] Chingombe P, Saha B, Wakeman RJ. Surface modification and characterization of coal-based activated carbon. Carbon 2005;43:3132–43.
[46] Mahapatra DM, Ramachandra TV. Algal biofuel: bountiful lipid from *Chlorococcum* sp. proliferating in municipal wastewater. Curr Sci 2013;105:47–55.
[47] Gai C, Zhang Y, Chen W-T, Zhang P, Dong Y. Thermogravimetric and kinetic analysis of thermal decomposition characteristics of low-lipid microalgae. Bioresour Technol 2013;150:139–48.
[48] Li L, Zhao N, Fu X, Shao M, Qin S. Thermogravimetric and kinetic analysis of *Spirulina* wastes under nitrogen and air atmospheres. Bioresour Technol 2013;140:152–7.
[49] Li D, Chen L, Chen S, Zhang X, Chen F, Ye N. Comparative studies on the pyrolytic and kinetic characteristics of a macroalga (*Sargassum thunbergii*) and a freshwater plant (*Potamogeton crispus*). Fuel 2012;96:185–91.
[50] Ye N, Li D, Chen L, Zhang X, Xu D. Comparative studies of the pyrolytic and kinetic characteristics of maize straw and the seaweed *Ulva pertusa*. PLoS ONE 2010;5:e12641.
[51] Rizzo AM, Prussi M, Bettucci L, Libelli IM, Chiaramonti D. Characterization of microalga Chlorella as a fuel and its thermogravimetric behavior. Appl Energy 2013;102:24–31.
[52] Peng W, Wu Q, Tu P, Zhao N. Pyrolytic characteristics of microalgae as renewable energy source determined by thermogravimetric analysis. Bioresour Technol 2001;80:1–7.
[53] Wu K, Liu J, Wu Y, Chen Y, Li Q, Xiao X, et al. Pyrolysis characteristics and kinetics of aquatic biomass using thermogravimetric analyzer. Bioresour Technol 2014;163:18–25.
[54] Li D, Chen L, Zhang X, Ye N, Xing F. Pyrolytic characteristics and kinetic studies of three kinds of red algae. Biomass Bioenergy 2011;35:1765–72.
[55] Li D, Chen L, Zhao J, Zhang X, Wang Q, Wang H, et al. Evaluation of the pyrolytic and kinetic characteristics of *Enteromorpha prolifera* as a source of renewable bio-fuel from the Yellow Sea of China. Chem Eng Res Des 2010;88:647–52.
[56] Li D, Chen L, Yi X, Zhang X, Ye N. Pyrolytic characteristics and kinetics of two brown algae and sodium alginate. Bioresour Technol 2010;101:7131–6.
[57] Verlaque M, Belsher T, Deslous-Paoli JM. Morphology and reproduction of Asiatic Ulva pertusa (Ulvales, Chlorophyta) in Thau Lagoon (France, Mediterranean Sea.). Cryptogam Algol 2002;23:301–10.
[58] Meng A, Zhou H, Qin L, Zhang Y, Li Q. Quantitative and kinetic TG–FTIR investigation on three kinds of biomass pyrolysis. J Anal Appl Pyrol 2013;104:28–37.
[59] Hossain ABMS, Salleh A, Boyce AN, Chowdhury P, Naqiuddin M. Biodiesel fuel production from algae as renewable energy. Am J Biochem Biotechnol 2008;4:250–4.
[60] Bridgwater AV. Principles and practice of biomass fast pyrolysis processes for liquids. J Anal Appl Pyrol 1999;51:3–22.
[61] Bae YJ, Ryu C, Jeon J-K, Park J, Suh DJ, Suh Y-W, et al. The characteristics of bio-oil produced from the pyrolysis of three marine macroalgae. Bioresour Technol 2011;102:3512–20.
[62] Uçar S, Karagöz S. The slow pyrolysis of pomegranate seeds: the effect of temperature on the product yields and bio-oil properties. J Anal Appl Pyrol 2009;84:151–6.
[63] Heo HS, Park HJ, Park, Yim JH, Sohn JM, Park J, et al. Influence of operation variables on fast pyrolysis of *Miscanthus sinesis var. Purpurascens*. Bioresour Technol 2010;1010:3672–7.
[64] Gilbert P, Ryu C, Sharifi VN, Swithenbank J. Tar reduction in pyrolysis vapours from biomass over a hot char bed. Bioresour Technol 2009;100:6045–51.
[65] Morf P, Hasler P, Nussbaumer T. Mechanisms and kinetics of homogeneous secondary reactions of tar from continuous pyrolysis of wood chips. Fuel 2002;81:843–53.
[66] Phan AN, Ryu C, Sharifi VN, Swithenbank. Characterization of slow pyrolysis products from segregated wastes for energy production. J Anal Appl Pyrol 2008;81:65–71.
[67] Yang H, Yan R, Chen H, Lee DH, Zheng C. Characteristics of hemicelluloses, cellulose and lignin pyrolysis. Fuel 2007;86:1781–8.
[68] Ross AB, Jones JM, Kubacki ML, Bridgeman T. Classification of macroalgae as fuel and its thermochemical behavior. Bioresour Technol 2008;99:6494–504.
[69] Ross AB, Anastasakis K, Kubacki M, Jones JM. Investigation of the pyrolysis behavior of brown algae before and after pre-treatment using PY-GC/MS and TGA. J Anal Appl Pyrol 2009;85:3–10.
[70] Fahmi R, Bridgwater AV, Darvell LI, Jones JM, Yates N, Thain S, et al. The effect of alkali metals on combustion and pyrolysis of *Lolium* and *Festuca* grasses, switchgrass and willow. Fuel 2007;86:1560–9.
[71] Raveendran K, Ganesh A, Khilar KC. Influence of mineral matter on biomass pyrolysis characteristics. Fuel 1995;74:1812–22.
[72] Hsisheng T, Wei YC. Thermogravimetric studies on the kinetics of rice hull pyrolysis and the influence of water treatment. Ind Eng Chem Res 1998;37:3806–11.